Risk factors for developing heel ulcers for bedridden patients: A finite element study

Clinical Biomechanics 78 (2020) 105094

Contents lists available at ScienceDirect

Clinical Biomechanics

journal homepage: www.elsevier.com/locate/clinbiomech

Risk factors for developing heel ulcers for bedridden patients: A finite element study

W.G.H. van Zwam, M.C. van Turnhout*, C.W.J. Oomens

Department of Biomedical Engineering, Eindhoven University of Technology, the Netherlands

ARTICLE INFO

Keywords:
Heel ulcers
Pressure ulcers
Heel pressures
Shear forces on heel
Deep tissue injury

ABSTRACT

Background: The heel is one of the most common sites of pressure ulcers and the anatomical location with the highest prevalence of deep tissue injury. Several finite element modeling studies investigate heel ulcers for bedridden patients. In the current study we have added the implementation of the calf structure to the current heel models. We tested the effect of foot posture, mattress stiffness, and a lateral calcaneus displacement to the contact pressure and internal maximum shear strain occurring at the heel.

Methods: A new 3D finite element model is created which includes the heel and calf structure. Sensitivity analyses are performed for the foot orientation relative to the mattress, the Young's modulus of the mattress, and a lateral displacement of the calcaneus relative to the other soft tissues in the heel.

Findings: The models predict that a stiffer mattress results in higher contact pressures and internal maximum shear strains at the heel as well as the calf. An abducted foot posture reduces the internal strains in the heel and a lateral calcaneus displacement increases the internal maximum shear strains. A parameter study with different mattress-skin friction coefficients showed that a coefficient below 0.4 decreases the maximum internal shear strains in all of the used loading conditions.

Interpretation: In clinical practice, it is advised to avoid internal shearing of the calcaneus of patients, and it could be taken into consideration by medical experts and nurses that a more abducted foot position may reduce the strains in the heel.

1. Introduction

A pressure ulcer is defined as: “a localized injury to the skin and underlying soft tissue, usually over a bony prominence, caused by sustained pressure, shear or a combination of these” (NPUAP, EPUAP, PPPIA, 2014). The heel and the sacrum are the most common locations for pressure ulcers (Campbell et al., 2010). A prevalence survey in the United States over a period of 16 years revealed that heel ulcers accounted for 24% of all bedridden hospital pressure ulcers and 23% of the total pressure ulcers in nursing homes (Bates-Jensen et al., 2018). In addition, the heel is the anatomical location accounting for 41% of all deep tissue injuries (Black, 2012).

Two damage mechanisms are believed to play a crucial role in pressure ulcer development (Oomens et al., 2013). The first mechanism involves tissue damage caused by pressure-induced ischemia. Reperfusion injury is sometimes mentioned as a mechanism that aggravates this ischemic damage. The second damage mechanism includes direct deformation damage beyond a certain tissue strain threshold level. This second mechanism could occur in the heel because the calcaneus bone has a relatively small surface with regard to the load it has to bear, making the heel vulnerable for high internal stresses (Langemo, 2015). Evidence for these damage mechanisms is mainly based on studies in skeletal muscle tissue. It is likely that similar mechanisms play a role in other soft tissues, but with different strain thresholds. Whether these mechanisms apply in heel ulcers is an open question.

Cichowitz et al. (Cichowitz et al., 2009) showed that the heel forms a cup-like structure consisting of skin overlying a shell of connective tissue containing fibrous septa, consequently connecting the skin to the calcaneus bone. Between these septa, islands of fat are located, which provide the shock-absorbing function of the heel. It is assumed that these septa form marginally vascularized compartments of fat, making them vulnerable for ischemia due to a buildup of compartment pressure in a situation similar to the compartment syndrome. Another hypothesis for heel ulcer development is that the panniculus muscle, located in the subcutaneous layer and the only muscle in the heel, is the primary side of injury (Cichowitz et al., 2009; Salcido et al., 1994). Clear evidence for these hypotheses is still lacking.

* Corresponding author.
E-mail address: M.C.v.Turnhout@tue.nl (M.C. van Turnhout).

https://doi.org/10.1016/j.clinbiomech.2020.105094
Received 13 September 2019; Accepted 12 June 2020

In clinical practice, the general consensus is that complete offloading of the heel is the most effective method for preventing heel ulcers (Butcher and Thompson, 2010). A simple and effective offloading method is the use of a pillow or cushion underneath the calf. However, maintaining the 'correct' cushion positioning is difficult and the heel tends to rapidly slip off the pillow, paradoxically increasing pressures rather than decreasing them (Junkin and Gray, 2009). Furthermore, this offloading method leads to increased sacral pressure and there is an increased chance for foot drop (Al-Majid et al., 2017). Also, complete heel offloading by removing the bed end is not always applicable for all patient groups and all types of mattresses. Heel offloading boot devices completely offload the heel while staying in place and reducing friction and shear. Solid evidence for their effectiveness is lacking. In addition these boots may be experienced as uncomfortable due to a bad fit, because they reduce patient mobility and increase the temperature and humidity of the heel micro environment (Clegg and Palfreyman, 2014).

Pressure has always been viewed as the main cause of pressure ulcers (Thomas, 2006), but since several years, shear- and friction forces have also been assumed to play a major role in the development of heel ulcers (Gefen, 2017). In healthcare settings often the head of the bed is elevated to improve the comfort of the patient and to facilitate respiratory functions. In this elevated position gravity causes downward forces that may result in a sliding movement of the patient in bed (Hermans and Call, 2015). This increases shear forces on the sacrum, but also at the heels of the patient. The shear forces can be reduced by placing patients in a semi-fowler position, but this is not always possible. The friction between the heel and supporting surface helps patients to prevent from moving, but also causes the calcaneus bone and connective tissue to move relative to the skin. This causes internal shear stresses and strains (Gefen et al., 2013). Similar effects occur in patients with leg spasms who dig their heels into the mattress (Black, 2004). In general, depending on the friction coefficient and the shear force at the interface we can have sliding friction or static friction. In both situations there is a "shear force" working at the interface, but in the case of sliding this force is usually smaller than during static friction. It is worthwhile to investigate the effects of shearing on the internal shear strains in the heel.

Apart from this 'shearing effect', foot posture and mattress type will affect internal stresses and strains occurring at the heel (Sopher et al., 2011). Gefen et al. created several foot models examining internal stresses and strains at the heel. These studies showed that atypical foot anatomies may form an extra risk factor to develop heel ulcers when compared to the average foot (Gefen, 2010). The same group found that strains and stresses were increased for a more abducted foot posture. This was also the case when the stiffness of the support stiffness was increased (Sopher et al., 2011). Heel dressings reduced strains and stresses located at the heel (Levy et al., 2015; Levy and Gefen, 2016). In these studies, the foot with a small part of the ankle was modeled and the total mechanical load on the heel was derived from assumptions based on the total weight of the foot. Luboz et al. included the total lower leg in their model. That study was focused on the influence of the calcaneus shape on the strains occurring at the heel (Luboz et al., 2015). A mean variation of maximum strain over 6.0 percentage points over 18 different morphologies was found. There was a clear influence of the cushion on which the leg was resting.

In the current study we included the calf in a finite element model of the heel. In a supine position, the calf makes contact with the support surface. Taking into account the consequence of the load distribution at the heel by implementing the calf into the finite element model may change the boundary conditions for the heel region of the model. The model is based on the geometry of one person and is focused on different positions of the foot, different values of the stiffness of the mattress, and on the effect of shear forces at the interface of the heel and the support surface.

The following questions are addressed:

1. How will foot posture and stiffness of the support affect the interface pressures and internal maximum shear strain occurring at the heel?
2. How do shear forces, resulting from different lateral displacements of the calcaneus with respect to the supporting surface, affect the internal maximum shear strain occurring at the heel?
3. How does a change in friction coefficient of the contacting surface affect the results found in 2?

2. Methods

2.1. Geometrical modeling

The geometry of the 3D lower leg model was based on data available from the Visible Korean Human project (http://vhk3.kisti.kr/) (Park et al., 2008). This site gives CT as well as MRI data. For the segmentation the CT data were used (better contrast). After cropping of the original image, the used image for segmentation was 494 × 281 pixels with a pixel size of 0.94 mm. The thickness of the slices was 1 mm. The lower leg model was from a male subject (age: 33 years; height: 164 cm, mass: 55 kg). Image segmentation was performed with the open source GIBBON toolbox (Moerman, 2018) in MATLAB (R2018b, the Mathworks, Matick, MA, USA). Contours of the calcaneus bone, Achilles tendon, and skin were imported into ABAQUS (2018, Dassault Systèmes Simulia corp., Providence, RI, USA) and lofted into a 3D solid body. The space between the skin, bone, and tendon tissues was filled with heel fat pad and muscle tissue. During the simulation, the leg model was supported by a cuboid mattress (Fig. 1(a)).

2.2. Mesh development

Meshing was performed with the mesh generator in ABAQUS. The lower leg consists of 26,199 quadratic tetrahedral elements with an increased mesh density at the heel region. Skin thickness was implemented to the model by adding 1974 quadratic wedge elements to the outer surface of the lower leg mesh with a 2 mm thickness, which is representative for heel skin thickness (Cichowitz et al., 2009). The support contains 2794 quadratic hexahedral elements with again an increased number of elements at the region of interest (Fig. 1(a)). A sensitivity analysis was performed to increase the mesh seed at the region of interest until the resulted changes of the contact pressure and maximum shear strain were below 5%.

The load on the leg in the model is a gravitational body force acting on every single material point. A good representation of internal deformations is only required in the heel, near the calcaneus. That is why that part is modeled in more detail. The internal structures (e.g. tibia) of the lower leg have a negligible effect on the internal deformations in the heel. That is why the lower leg is modeled as a single structure.

2.3. Material properties

The lower leg model represents five different components: calcaneus bone, Achilles tendon, heel fat pad, skin, and muscle tissue. Skin and fat tissue were modeled with a first-order hyperelastic Ogden model with the following constitutive material behavior formulation:

$$U = \frac{2\mu}{\alpha^2}(\bar{\lambda}_1^{\alpha} + \bar{\lambda}_2^{\alpha} + \bar{\lambda}_3^{\alpha}) + \frac{1}{D}(J-1)^2 \quad (1)$$

$$\bar{\lambda}_i = J^{-\frac{1}{3}}\lambda_i \quad (2)$$

$$J = \det(\mathbf{F}) \quad (3)$$

with U the strain energy density, μ the shear modulus, α a dimensionless material parameter, λ_i (i = 1,2,3) the principal stretch ratios, D an incompressibility parameter, J the ratio between the deformed volume and the initial volume, and $\mathbf{F}$ the deformation gradient tensor. The calcaneus, Achilles tendon and muscle were modeled as an isotropic

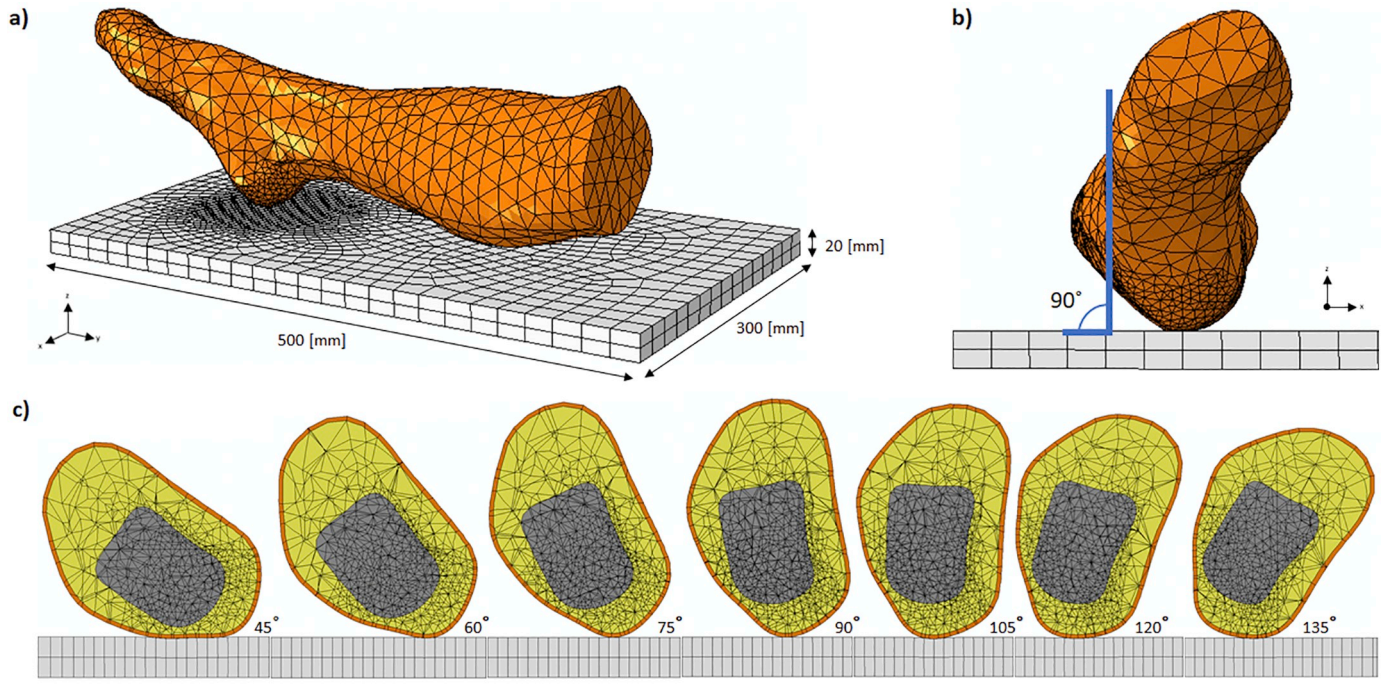

Fig. 1. The FE model of the lower leg. Fig. 1(a) shows the total lower leg resting on a mattress with increased mesh density at the contact surfaces located at the heel. Fig. 1(b) shows the model of the heel with a 90°-orientation relative to the mattress. In Fig. 1(c), cross sections of the transverse plane at the level of the calcaneus are presented for the different heel angels which are tested in the foot posture sensitivity analysis: fat tissue (yellow), skin tissue (orange), bone tissue (dark gray), support (white). (For interpretation of the references to colour in this figure legend, the reader is referred to the web version of this article.)

Table 1
Mechanical properties of the FE model adopted from literature.

Tissue\material	μ [MPa]	α [−]	D [mm^2/N]	E [kPa]	ν [−]
Skin [5,6]	50	2.3	0.81	–	0.49
Heel fat pad [7,8]	16	6.82	2.51	–	0.49
Bone [9]	–			7.30×10^6	0.30
Achilles Tendon [10]	–	–		8.16×10^5	0.49
Muscle [5]	–	–		60	0.49
Mattress[11]	–	–		50	0.30

[5] (Luboz et al., 2015).
[6] (Levy et al., 2015).
[7] (Spears et al., 2007).
[8] (Erdemir et al., 2006).
[9] (Akrami et al., 2018).
[10] (Wren et al., 2001).
[11] (Levy et al., 2015).

linear elastic material. Table 1 shows the material properties of the finite element model, which were adopted from literature. The lower leg is supported by a flat mattress with linear-elastic mechanical properties, with Young's modulus value $E = 50$ kPa and a Poisson's ratio $\nu = 0.3$ which is in the range of typical hospital mattress values (Levy et al., 2015).

2.4. Boundary conditions

To model the interaction between the lower leg and mattress, a lower leg displacement in z-direction was prescribed until the leg makes contact with the support. From there, the lower leg with a total mass of 3.36 kg was subjected to a body force as a result of the applied gravitation acceleration of -9.81 m/s^2. A static contact friction coefficient of 0.4 was applied for the skin-support contact (Zhang and Mak, 1999).

2.5. Protocol of simulations

Different sensitivity analyses were performed to look at the effects of mattress stiffness, foot posture and shear forces at the interface between heel and contact surface. In all simulations one parameter was varied, while the other parameters were kept at the values from the reference model.

In the first series the Young's modulus of the mattress was varied (10 kPa to 100 kPa with 10 kPa increments, 200 kPa, and 400 kPa).

Next, foot posture was varied by orienting the lateral aspect of the heel relative to the mattress from 45° to 135° with 15° increments (Fig. 1(b)(c)).

For assessment of the shear force, a calcaneus displacement was prescribed in y-direction (0 mm to 10 mm with 2 mm increments) with a no sliding condition at the interface (= infinite friction).

The effect of the friction coefficient was tested by setting a 5 mm calcaneus displacement (Levy et al., 2015) and varying the friction coefficient value between 0.0 (frictionless) and 1.0 (very high friction) with increments of 0.1.

2.6. Outcome measures

For each simulation, the maximum shear strain was determined for the region of interest in the heel. This heel region of interest (where the mesh density is highest, Fig. 1), has a total volume of 5.34×10^5 mm^3. The maximum shear strain was calculated according to Eq. (4):

$$\gamma_{max} = \frac{1}{2}(\varepsilon_1 - \varepsilon_3) \tag{4}$$

with ε_1 the maximum principal logarithmic strain and ε_3 the minimum principal logarithmic strain. These values were calculated at the integration points and exported from Abaqus. Also the associated volume of the integration points was determined to quantify the tissue volume with maximum shear strains in a specific strain range. For the sensitivity analysis of mattress stiffness and foot posture, the contact pressure at the heel and calf was obtained. This pressure was calculated

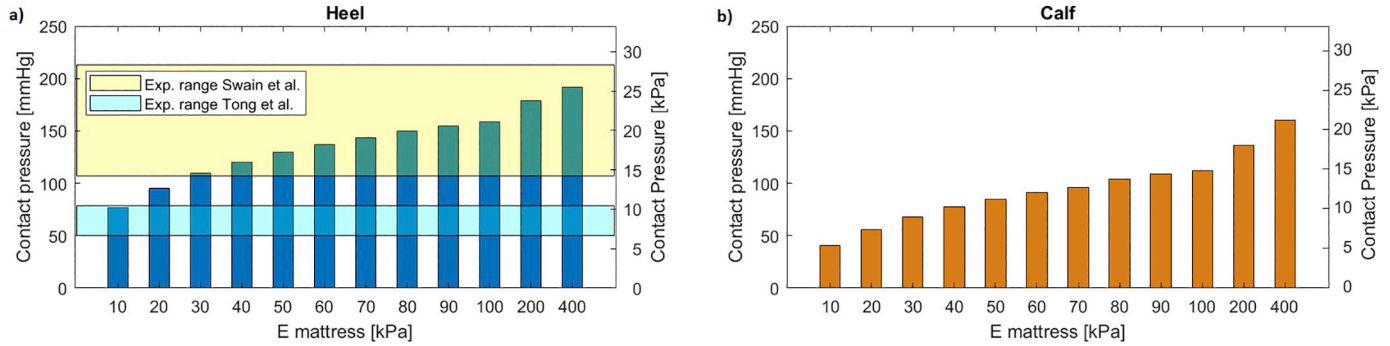

Fig. 2. Contact pressures for different mattress Young's moduli at a 90°-oriented foot posture. Fig. 2(a): heel contact pressures. Fig. 2(b): calf contact pressures. For both figures, values are represented in mmHg (left y-axis) and kPa (right y-axis).

by dividing the nodal values of contact normal force by the contact area. To compare the values with performed experimental work, these values were calculated and summed up over a surface area comparable to a 18 mm pressure sensor (MK III; Talley Medical, Romsey, UK) used in experimental studies (Swain et al., 1993).

3. Results

3.1. Sensitivity analysis: mattress stiffness

Fig. 2 represents calculated contact pressure values at the skin surface of the heel and calf for a 90°-oriented foot position. It was clear that for an increasing mattress Young's modulus, both heel (Fig. 2(a)) and calf (Fig. 2(b)) contact pressures increase. Heel contact pressures were generally larger than calf contact pressures for similar mattress Young's moduli. In the shaded areas, a comparison was made between our finite element model values and experimental studies examining heel ulcers (Swain et al., 1993; Tong et al., 2016). For Young's moduli from 30 kPa, heel contact pressures were within the range of values found by the experimental study of Swain et al. Only the simulation with a mattress Young's modulus of 10 kPa showed heel contact pressures in the range of contact pressure values obtained by Tong et al.

Fig. 3(a) shows the distribution of maximum shear strains ranging from 0.05–0.40 for different mattress Young's moduli at the region of interest at the heel, the heel fat pad and skin tissue around the calcaneus. In Fig. 3(b), a magnification of the strains between 0.25 and 0.40 is presented. There is a clear trend that for increased mattress stiffnesses also the volume of soft tissue experiencing larger strains will increase.

3.2. Sensitivity analysis: foot posture

The model predicted the highest contact pressure (138 mmHg – 18 kPa) for a foot orientation of 135° for the heel (Fig. 4(a)). A foot orientation of 45° and 60° led to lower heel contact pressures compared to the more adducted foot postures (105°, 120° and 135°). For the region of interest at the calf, the lowest contact pressure (32 mmHg – 4.3 kPa) was found at the most abducted foot position (45°). The 90° position caused the highest contact pressures at the calf (85 mmHg – 11.3 kPa, Fig. 4(b)).

For these different foot postures different internal strain distributions in the heel were predicted. For all foot positions, the largest values of γ_{max} were found at the fat-calcaneus interface. However, for each

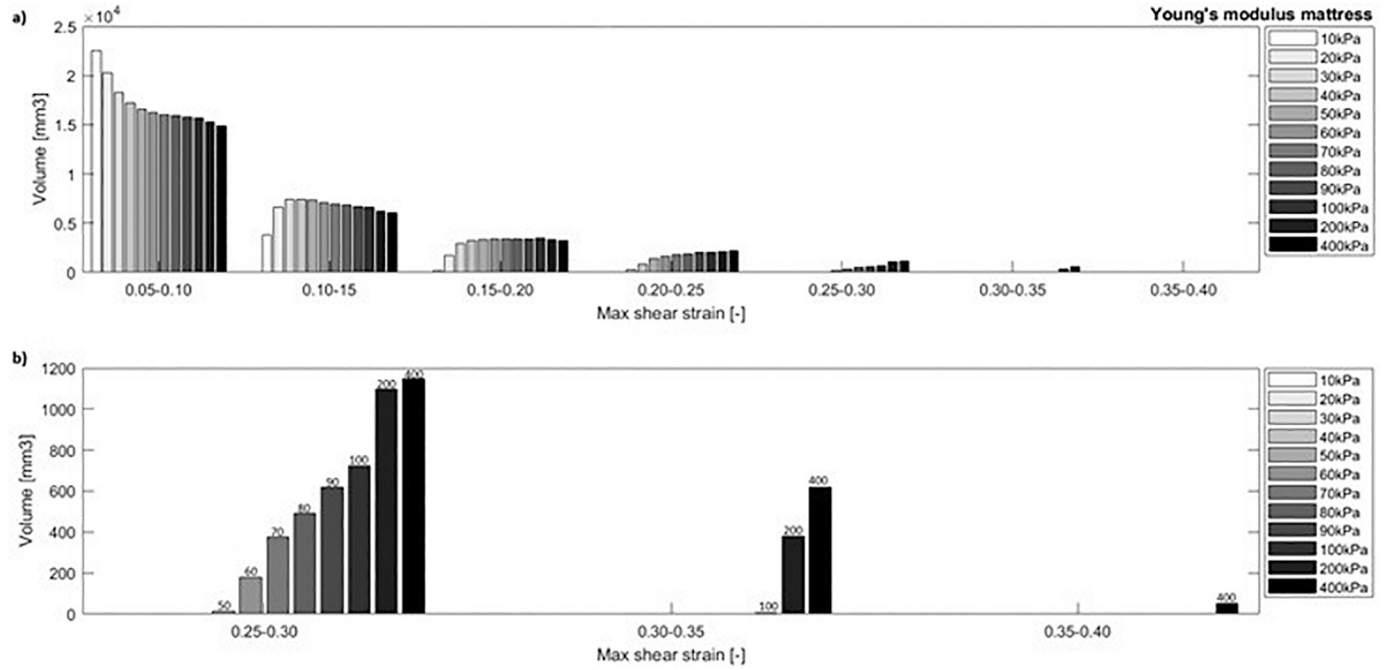

Fig. 3. Maximum shear strain distribution for different mattress Young's moduli at the heel region of interest for a 90°-oriented foot position. Total volume of heel region of interest is 5.34×10^5 mm^3. Strains from 0.00–0.05 are omitted in Fig. 3(a) to show a clear overview of the strain region of interest. Fig. 3(b) is a magnification of the highest three shear strain ranges from Fig. 3(a). Labels are added to the top of the bars which represents the mattress stiffness value [kPa].

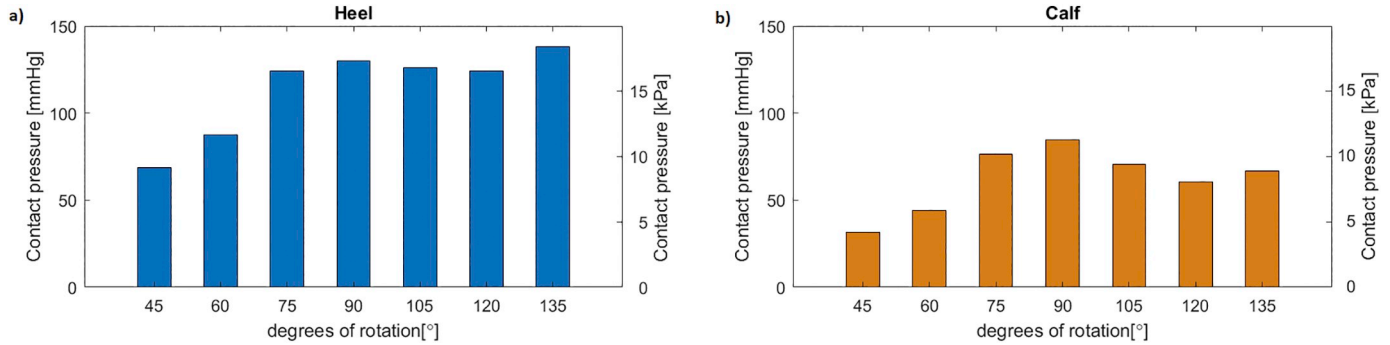

Fig. 4. Contact pressures at the heel (Fig. 4(a)) and calf (Fig. 4(b)) for different foot postures. For both figures, values are represented in mmHg (left y-axis) and kPa (right y-axis).

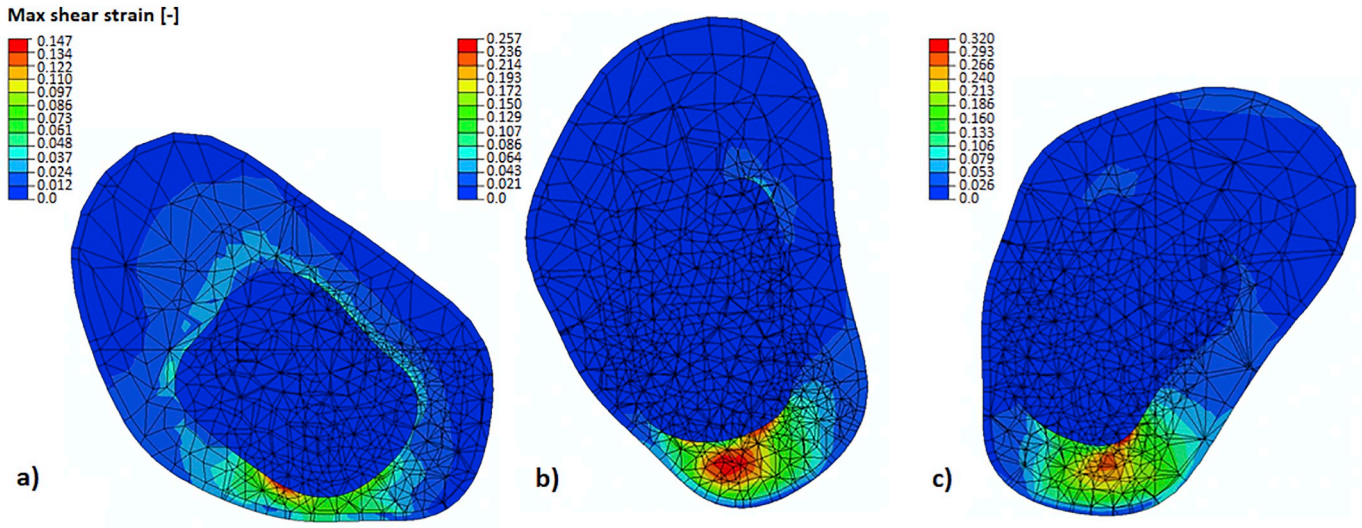

Fig. 5. Distributions of maximum shear strain nodal values in the transverse plane at the slice where the highest maximum shear strains were found for the 45°(Fig. 5(a)), 90° (Fig. 5(b)), and 135° (Fig. 5(c)) foot orientation; mattress Young's modulus: 50 kPa.

foot posture, these peak values were found at a different locations in the heel pad region below the calcaneus (Fig. 5). Not only was the peak strain location different, also the magnitude of the strains differ between the simulations. In Fig. 6(a), we show a histogram with maximum shear strain values from 0.05–0.35 for a heel resting on a support with a Young's modulus of 50 kPa. We found that a more adducted foot position results in higher shear strains at the tissue beneath the calcaneus bone (Fig. 6b).

3.3. Sensitivity analysis: lateral displacement with and without sliding

Internal shear strain values between 0.10 and 0.40 are presented in Fig. 7(a) for the case with infinite friction and a lateral displacement of the leg of 0 to 10 mm. For the larger strain (0.20–0.40) we found a clear trend that the volume of soft tissue in this strain range increases with an increased lateral displacement (Fig. 7(b)).

Fig. 8 shows the results of the simulation with a lateral sliding of 5 mm but with varying friction coefficients. For friction coefficient values below 0.3, an increased soft tissue volume was obtained in the lower strain range (0.10–0.15) compared to the friction coefficient values of 0.3–1.0 (Fig. 8). For the maximum shear strain range from 15% up to 30%, friction coefficient values below 0.5 had a lower soft tissue volume in this specific strain range compared to the values from 0.5–1.0. For the friction coefficient values from 0.5–1.0, we did not find a clear difference between the volume in the specific strain range.

4. Discussion

In the present work, a heel finite element model including the calf is developed to study the influence of foot posture, mattress stiffness and a lateral calcaneus displacement on the risk of HU formation.

Contact pressures at the heel were obtained in the range of 10 kPa–25 kPa depending on the mattress Young's modulus and foot orientation relative to the mattress (Fig. 2; Fig. 4). The contact pressures are in the same range as found in the experimental studies of Swain et al. (Swain et al., 1993) which examined heel contact pressures for bedridden patients (Fig. 2). Tong et al. (Tong et al., 2016) did similar studies but found lower pressure values. In our study such low values are only found when a very small mattress stiffness ($E_{mattress}$ = 10 kPa) is used. It is not known what the exact Young's modulus of the support surface was in those experimental studies because they were not presented. The values used in our stiffness sensitivity analysis are in the standard range of a hospital bed (Levy et al., 2015).

Peak internal maximum shear strain values were found around 15%–40%, again depending on foot posture and support stiffness (Fig. 3; Fig. 7). For a stiffer mattress and a more adducted foot posture, the contact pressures and internal strain values increase. The effect of increasing contact pressures and internal strain values for a stiffer mattress was also seen in studies of Sopher et al. and Luboz et al. (Sopher et al., 2011; Luboz et al., 2015). In the current finite element model, the 90° position shows higher contact pressures and internal maximum shear strains compared to the more abducted foot orientation

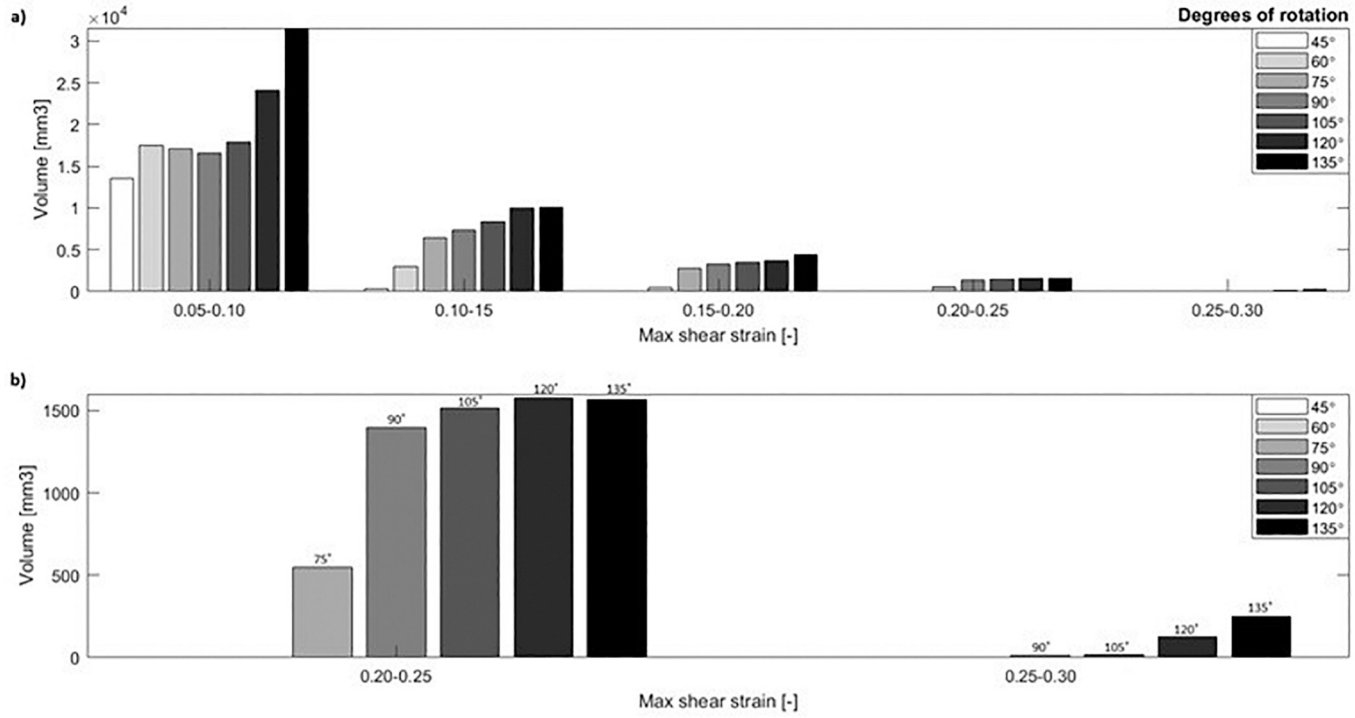

Fig. 6. Maximum shear strain distribution for different foot postures at the heel region of interest for a mattress Young's modulus of 50 kPa. Fig. 6(b) is a zoom of the last two shear strain ranges from Fig. 6(a). Total volume of heel region of interest is 5.34×10^5 mm^3. Strains from 0.00–0.05 are omitted in Fig. 6(a) to show a clear overview of the strain region of interest.

of 60°. This is in accordance with the experimental study by Tong et al. (Tong et al., 2016), who examined contact pressures for different foot postures. However, this is a different result than obtained in another finite element study examining heel ulcers (Sopher et al., 2011). That study showed higher internal fat pad strains and contact pressures for the abducted foot position of 60°. Apparently, introducing the calf in the model has a large influence on these internal strains. Our current model shows that for a more abducted foot position (45°, 60°), the contact pressures and internal strains will decrease compared to the more adducted foot positions.

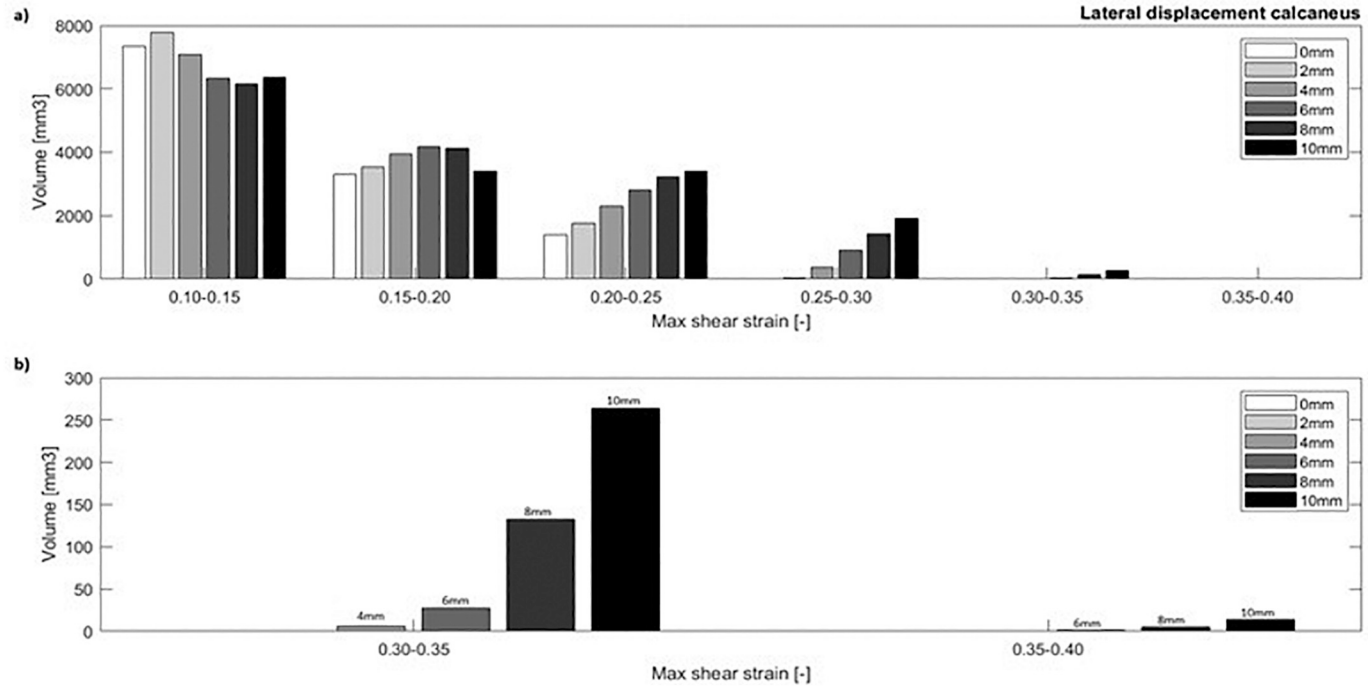

Fig. 7. Maximum shear strain distribution for different lateral calcaneus displacements relative to the soft tissues at the heel region of interest at a support with Young's modulus of 50 kPa. All simulations were done under no slip conditions. Fig. 7(b) is a magnification of the last two shear strain ranges from Fig. 7(a). Total volume of heel region of interest is 5.34×10^5 mm^3. Strains from 0.00–0.10 are omitted in Fig. 7(a) to show a clear overview of the strain region of interest.

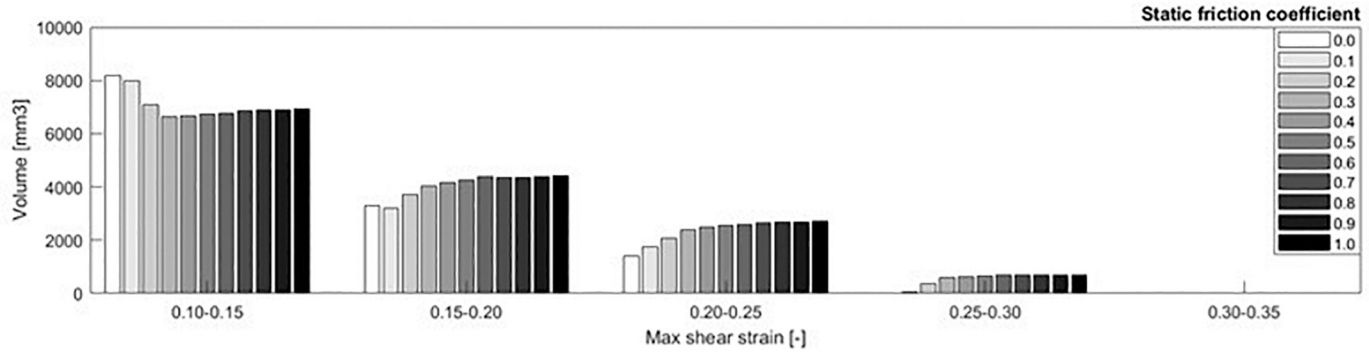

Fig. 8. Maximum shear strain distribution for different static friction coefficients between skin and mattress for a 5 mm lateral calcaneus displacements relative to the other soft tissues at the heel region of interest. Total volume of heel region of interest is 5.34×10^5 mm^3. Strains from 0.00–0.10 are omitted in Fig. 8 to show a clear overview of the strain region of interest.

A lateral displacement of the calcaneus relative to the soft tissues in the heel results in higher internal maximum shears strains (Fig. 7). A similar effect was seen in studies of Levy et al. (Levy et al., 2015; Levy and Gefen, 2016). Varying the static friction coefficient between the hospital mattress and skin tissue affects the internal strains occurring at the heel during the shearing effect (Fig. 8). At a friction coefficient below 0.4 there is a large influence on the volume of tissue that experiences high strains. Variation of the friction coefficient with values above 0.4 does not influence the mechanical state of the tissue much. Probably the reason for this is that higher friction coefficients lead to a no-slip condition.

This lower leg FE model does not include the ankle and knee joint. The upper leg, and especially the buttock, is involved in the load distribution of the total leg (Lee et al., 2017) and may affect the contact pressures and shear strains at the heel. The ankle joint is also responsible for the plantar flexion movement of the foot, which seems to affect the internal strains at the heel (Levy and Gefen, 2016). Implementation of two extra joints will make the model considerably more complex, but it will certainly improve the ability to describe the loading on the heel more accurate.

The selected CT data used for this model were from a 33-year-old Korean male which may not be representative for the risk group of patients experiencing heel ulcerations although the observed trends may be the same for other subjects. In a future study other patient morphologies should be taken into account to test if it is defendable to draw conclusions from findings based on our study. The mechanical properties chosen for our materials in the model show a large variety in literature and can also differ per person. A linear elastic material law was chosen for bone, Achilles tendon and muscle tissue. Because of small rotations of the bone and other soft tissues in the calve this can be defended, especially because we focus on the contact pressures and shear strains in the heel and the calve is mainly included because of its weight and global shape. In addition, our purpose was to identify trends and not to accurately predict contact pressures and shear strains in absolute terms. However, the accuracy will certainly improve when a constitutive law is used that accounts for geometrical nonlinearities.

If the finding that an abducted foot position will reduce the shear strains at heel level holds (more validation is necessary), this could be used to improve ways to prevent heel ulcers. This could be done by developing new devices to unload the heel or by different supporting procedures of the foot after repositioning.

It is clear that shear forces on the heel, because of a lateral displacement, increase the internal shear strains in the heel pad. This will have an effect on the risk for pressure ulcers in the heel. It does not only play a role when the skin “sticks” to the supporting bed sheet, but also in case the skin “slides” along the bed sheet. In both cases shear forces are present, although in the case of sliding the shear forces are lower. This has some major consequences for the clinic. It is important to be aware of these shear forces, for example when the head of the bed is lifted or when moving patients. This may be a reason to adapt procedures for patient handling. Recently a number of publications appeared in literature about the positive effect of heel dressings to prevent pressure ulcers. Current heel dressings in a clinical setting are able to reduce the friction coefficient value between heel and bed sheet below 0.4 (Nakagami et al., 2006). The findings obtained in our research indicate that an additional heel dressing, applied to decrease the friction coefficient, can indeed reduce the soft tissue strain in the heel. This effect was also seen by Levy et al. (Levy et al., 2015; Levy and Gefen, 2016).

5. Conclusions

To conclude, this lower leg model seems to provide a realistic reproduction of the contact pressures and internal strains occurring at heel level, although more validation is necessary. The models predict that an abducted foot position will reduce the contact pressures and shear strains at the heel, just as a mattress with a lower Young's modulus. We further found that an internal lateral displacement of the calcaneus bone relative to the surrounded soft tissues as a result of shear forces at the interface, leads to increased internal shear strains in the models.

Declaration of Competing Interest

None.

Appendix A. Supplementary data

Supplementary data to this article can be found online at https://doi.org/10.1016/j.clinbiomech.2020.105094.

References

Akrami, M., Qian, Z., Zou, Z., Howard, D., Nester, C.J., Ren, L., 2018. Subject-specific finite element modelling of the human foot complex during walking: sensitivity analysis of material properties, boundary and loading conditions. Biomech. Model. Mechanobiol. 17 (2), 559–576. https://doi.org/10.1007/s10237-017-0978-3.

Al-Majid, S., Vuncanon, B., Carlson, N., Rakovski, C., 2017. The effect of offloading heels on sacral pressure. AORN J. 106 (3), 194–200. https://doi.org/10.1016/j.aorn.2017.07.002.

Bates-Jensen, B.M., McCreath, H.E., Nakagami, G., Patlan, A., 2018. Subepidermal moisture detection of heel pressure injury: the pressure ulcer detection study outcomes. Int. Wound J. 15 (2), 297–309. https://doi.org/10.1111/iwj.12869.

Black, J., 2004. Preventing heel pressure ulcers. Nursing 34 (11), 17. https://doi.org/10.1097/WON.0000000000000181.

Black, J., 2012. Technology and product reviews TECHNOLOGY UPDATE : Preventing pressure ulcers occurring on the heel. 3(3). pp. 1–4.

Butcher, M., Thompson, G., 2010. Can the use of dressing materials actually prevent pressure ulcers: presenting the evidence. Wounds UK 6 (1), 119–125.

Campbell, K.E., Woodbury, M.G., Houghton, P.E., 2010. Implementation of best practice

in the prevention of heel pressure ulcers in the acute orthopedic population. Int. Wound J. 7 (1), 28–40. https://doi.org/10.1111/j.1742-481X.2009.00650.x.
Cichowitz, A., Pan, W.R., Ashton, M., 2009. The heel: anatomy, blood supply, and the pathophysiology of pressure ulcers. Ann. Plast. Surg. 62 (4), 423–429. https://doi.org/10.1097/SAP.0b013e3181851b55.
Clegg, R., Palfreyman, S., 2014. Of heel pressure ulcers : a review, (August 2018). pp. 20–25. https://doi.org/10.12968/bjon.2014.23.Sup20.S4.
Erdemir, A., Viveiros, M.L., Ulbrecht, J.S., Cavanagh, P.R., 2006. An inverse finite-element model of heel-pad indentation. J. Biomech. 39 (7), 1279–1286. https://doi.org/10.1016/j.jbiomech.2005.03.007.
Gefen, A., 2010. The biomechanics of heel ulcers. J. Tissue Viabil. 19 (4), 124–131. https://doi.org/10.1016/j.jtv.2010.06.003.
Gefen, A., 2017. Why is the heel particularly vulnerable to pressure ulcers? Br. J. Nurs. *26* (Sup20), S62–S74. https://doi.org/10.12968/bjon.2017.26.sup20.s62.
Gefen, A., Farid, K., Ira, S., 2013. PL a review of deep tissue injury PL. Ostomy Wound Manage 59 (2), 26–35.
Hermans, M.H., Call, E., 2015. Failure to reposition after sliding down in bed increases pressure at the sacrum and heels. Wounds 27 (7), 191–198.
Junkin, J., Gray, M., 2009. Are pressure redistribution surfaces or heel protection devices effective for preventing heel pressure ulcers? J. Wound Ostomy Contin. Nursing 36 (6), 602–608. https://doi.org/10.1097/WON.0b013e3181be282f.
Langemo, D., 2015. Heel Pressure Ulcers : 2014 International Pressure Ulcer Prevention & Treatment Guidelines Heel Anatomy & Physiology. pp. 1–22.
Lee, W., Won, B.H., Cho, S.W., 2017. Finite element modeling for predicting the contact pressure between a foam mattress and the human body in a supine position. Comp. Methods Biomech. Biomed. Eng. 20 (1), 104–117. https://doi.org/10.1080/10255842.2016.1203421.
Levy, A., Gefen, A., 2016. Computer Modeling studies to assess whether a prophylactic dressing reduces the risk for deep tissue injury in the heels of supine patients with diabetes. Ostomy Wound Manage 62 (4), 42–52.
Levy, A., Frank, M.B.O., Gefen, A., 2015. The biomechanical efficacy of dressings in preventing heel ulcers. J. Tissue Viabil. 24 (1), 1–11. https://doi.org/10.1016/j.jtv.2015.01.001.
Luboz, V., Perrier, A., Bucki, M., Diot, B., Cannard, F., Vuillerme, N., Payan, Y., 2015. Influence of the Calcaneus Shape on the Risk of Posterior Heel Ulcer Using 3D Patient-Specific Biomechanical Modeling. Ann. Biomed. Eng. 43 (2), 325–335. https://doi.org/10.1007/s10439-014-1182-6.
Moerman, K.M., 2018. GIBBON: the geometry and image-based bioengineering add-on. J. Open Source Software 3 (22), 506. https://doi.org/10.21105/joss.00506.
Nakagami, G., Sanada, H., Konya, C., Kitagawa, A., Tadaka, E., Tabata, K., 2006. Comparison of two pressure ulcer. J. Wound, Ostomy Contin. Nursing 33 (3), 267–272 (5).
National Pressure Ulcer Advisory Panel, European Pressure Ulcer Advisory Panel, & Pan Pacific Pressure Injury Alliance, 2014. Prevention and Treatment of Pressure Ulcers: Quick Reference Guide. Guidelines. Retrieved from. http://www.npuap.org/wp-content/uploads/2014/08/Quick-Reference-Guide-DIGITAL-NPUAP-EPUAP-PPPIA-Jan2016.pdf.
Oomens, C.W.J., Zenhorst, W., Broek, M., Hemmes, B., Poeze, M., Brink, P.R.G., Bader, D.L., 2013. A numerical study to analyse the risk for pressure ulcer development on a spine board. Clin. Biomech. 28 (7), 736–742. https://doi.org/10.1016/j.clinbiomech.2013.07.005.
Park, J.S., Jung, Y.W., Lee, J.W., Shin, D.S., Chung, M.S., Riemer, M., Handels, H., 2008. Generating useful images for medical applications from the visible Korean human. Comput. Methods Prog. Biomed. 92 (3), 257–266. https://doi.org/10.1016/j.cmpb.2008.07.007.
Salcido, R., Donofrio, J.C., Fisher, S.B., LeGrand, E.K., Dickey, K., Carney, J.M., ... Liang, R., 1994. Histopathology of pressure ulcers as a result of sequential computer-controlled pressure sessions in a fuzzy rat model. Adv. Wound Care 7 (5), 23–24.
Sopher, R., Nixon, J., McGinnis, E., Gefen, A., 2011. The influence of foot posture, support stiffness, heel pad loading and tissue mechanical properties on biomechanical factors associated with a risk of heel ulceration. J. Mech. Behav. Biomed. Mater. 4 (4), 572–582. https://doi.org/10.1016/j.jmbbm.2011.01.004.
Spears, I.R., Miller-Young, J.E., Sharma, J., Ker, R.F., Smith, F.W., 2007. The potential influence of the heel counter on internal stress during static standing: a combined finite element and positional MRI investigation. J. Biomech. 40 (12), 2774–2780. https://doi.org/10.1016/j.jbiomech.2007.01.004.
Swain, I., Stacey, P., Dunford, C., Nichols, R., 1993. Evaluation, PS1 Foam Mattresses. Medical Devices Agency, Department of Health.
Thomas, D.R., 2006. Prevention and Treatment of Pressure Ulcers. Clinical practice in long-term care 7 (1), 46–59. https://doi.org/10.1016/j.clinbiomech.2015.11.006.
Tong, S.F., Yip, J., Yick, K.L., Yuen, M.C.W., 2016. Effects of different heel angles in sleep mode on heel interface pressure in the elderly. Clin. Biomech. 32, 229–235. https://doi.org/10.1016/j.clinbiomech.2015.11.006.
Wren, T.A.L., Yerby, S.A., Beaupr, G.S., Carter, D.R., Beaupré, G.S., 2001. Mechanical properties of the human achilles tendon. Clin. Biomech. 16 (3), 245–251.
Mak, A.F.T., Zhang, M., 1999. *In vivo* friction properties of human skin. Prosthetics Orthot. Int. 30 (3), 279–285. https://doi.org/10.3109/03093649909071625.